· Article · Advances in Polar Science

doi:10.3724/SP.J.1085.2011.00143 September 2011 Vol.22 No.3 143–152

Thermodynamic processes of lake ice and landfast ice around Zhongshan Station, Antarctica

LEI RuiBo[1*], LI ZhiJun[2], ZHANG ZhanHai[1] & CHENG YanFeng[1]

[1]Polar Research Institute of China, Shanghai 200136, China;

[2]State Key Laboratory of Coastal and Offshore Engineering, Dalian University of Technology, Dalian 116024, China

Received July 27, 2011; accepted August 16, 2011

Abstract Thermodynamic processes of ice in three lakes and landfast ice around Zhongshan Station, Antarctica, were observed in 2006. The mass balance of lake ice was compared with that of landfast ice. The responses of lake ice and sea ice temperatures to the local surface air temperature are explored. Vertical conductive heat fluxes at varying depths of lake ice and sea ice were derived from vertical temperature profiles. The freeze up of lake ice and landfast ice occurred from late February to early March. Maximum lake ice thicknesses occurred from late September to early October, with values of 156–177 cm. The maximum sea ice thicknesses of 167–174 cm occurred relatively later, from late October to late November. Temporal variations of lake ice and landfast ice internal temperatures lagged those of air temperatures. High-frequency variations of air temperature were evidently attenuated by ice cover. The temporal lag and the high-frequency attenuation were greater for sea ice than for lake ice, and more distinct for the deeper ice layer than for the upper ice layer. This induced a smaller conductive heat flux through sea ice than lake ice, at the same depth and under the same atmospheric forcing, and a smoother fluctuation in the conductive heat flux for the deeper ice layer than for the upper ice layer. Enhanced desalination during the melt season increased the melting point temperature within sea ice, making it different from fresh lake ice.

Keywords **Sea ice, lake ice, thermodynamics, thickness, temperature, Antarctica**

Citation: Lei R B, Li Z J, Zhang Z H, et al. Thermodynamic processes of lake ice and landfast ice around Zhongshan Station, Antarctica. Adv Polar Sci, 2011, 22: 143–152, doi: 10.3724/SP.J.1085.2011.00143

0 Introduction

Sea ice that grows attached to the coast, the front of a glacier tongue or ice shelf, or a grounded iceberg, is defined as landfast ice. Because of its immovability, it has long been considered as an ideal measure of local climate change, similar to lake ice[1−4]. RADARSAT ScanSAR data has shown that landfast ice constitutes about 28% by volume of sea ice in the Antarctic sector of 75°–170°E, during November[5]. Because of its longer ice season and larger thickness compared to pack ice in the same region, landfast ice cannot be neglected when evaluating the role of Antarctic sea ice within the climate system. Lake ice thermodynamic processes can influence the biological, chemical and physical processes of lake systems. For example, the duration and composition of lake ice controls the seasonal heat budget of lake systems[6]. Lake ice modulates underwater light conditions[7], mixing processes[8], and nutrient recycling and oxidation[9]. Ice breakup strongly influences plankton dynamics[10] and winter fish kill[11].

Lake coverage in the Larsemann Hills region, where Zhongshan Station is located, is 3.15%, representing a total area of 6.3 km^2. The lakes are mainly fed by snowmelt runoff[12], and they may generally freeze over completely

*Corresponding author (email: leiruibo@pric.gov.cn)

by ice in mid to late February, and become ice free by the end of December to mid January of the following year. The ice season of lakes close to the continental ice sheet is relatively longer[12]. There are several islands off Zhongshan, and the nearby bathymetry is greatly undulated[13]. Therefore, a large number of icebergs, including those calved from Dålk Glacier, tend to ground offshore from the Larsemann Hills. Landfast ice off Larsemann Hills usually breaks off in early summer, often because of contemporaneous high wind speeds, monthly peak tides, and/or penetrating ocean swell[14]. Freeze up usually takes place in February or March. Occasionally, a small portion of landfast ice may survive through summer to form multi-year sea ice within a narrow bay or fjord, both of which provide protection from ocean swell and wind fetch[15]. Zhongshan Station can thus provide an ideal supporting base for year-round synchronous investigations of lake ice and landfast ice thermodynamic processes.

Thermodynamic processes of ices on three lakes in the Larsemann Hills and landfast ice around Zhongshan Station were observed through 2006. Snow thermal conductivity and oceanic heat flux under ice cover were estimated based on in-situ snow and landfast ice mass balance data[16]. The contributions of snow cover to the landfast ice thermodynamic processes were explored based on comparison between the data from 2005 and 2006[17]. The principal object of the current study is to compare the thermodynamic processes of landfast ice with those of lake ice, forced by the same local meteorological conditions.

1 Field work and data

Meteorological data were obtained from a manned weather station, one kilometer inland from the experimental site, at 14 m above sea level. During 2006 the mean air temperature was –9.6°C representing a positive anomaly of 0.4°C compared to the mean from 1989 to 2006. The lowest monthly mean air temperature occurred in July (–18.6°C), and the highest in January (0.4°C). The lowest annual air temperature was –30.2°C, on 28 July, and the highest was 7.6°C, on 5 January. Surface winds at Zhongshan were generally from the north or east (about 77.1% of the time).

Lake ice observations were made at Lakes Mochou, Tuanjie and Progress (Figure 1). Lake Mochou was the site of primary investigation. Morphological properties of these lakes are shown in Table 1. Lake Progress is near the continental ice sheet, whereas Lakes Mochou and Tuanjie are near the coast. A water volume of about 60 m^3 per month was supplied from Lake Mochou to Zhongshan Station, through a pump fixed on the bottom of the lake, about 10 m from its eastern shore. On 10 March, three hot wire thickness gauges were deployed in a triangular configuration at the centre of Lake Mochou, for monitoring ice and snow thicknesses. The gauges had a precision of ±0.5 cm. Details on this gauge may be found in Lei et al.[18]. Measurements were taken from 17 March to 30 October, at a frequency of one to three days. On 10 April, a thermistor string was deployed among the hot wire thickness gauges, to measure the vertical temperature profile from ice to water. The thermistors were assembled with PT100 sensors at level A, with a precision of ±0.1°C. The coherence of these sensors was controlled by selecting those that read within ±0.05 K of each other during calibration prior to the deployment. The vertical spacing of the sensors was 6 cm for depths between 0 to –144 cm, and 12 cm for depths between –144 to –204 cm. Measurements were taken from 18 April to 20 October, at an interval of 30 min. Snow and ice thicknesses at Lakes Tuanjie and Progress were measured by making a hole with a drill with a 5-cm diameter stainless steel auger. This was done every 5–10 days at three holes, from 15 March to 17 November. The accuracy of the drill-hole method was ±0.5 cm.

Landfast ice measurements were made at three sites,

Table 1 Morphological properties of the lakes[12]

Lake	Altitude/m	Max. depth/m	Area/m^2	Max. length/m	Max. width/m
Mochou	10	3.8	5 000	50	30
Tuanjie	5	4.5	50 000	255	225
Progress	65	34	105 000	600	300

as shown in Figure 1. These were located off the northeast coast of the Mirror peninsula (S1), off its northern coast (S2), and to the south of Nella Fjord (S3). The primary investigated site was S2. The shortest distances from the S1–S3 sites to the coast are 400 m, 280 m and 150 m, respectively. The ocean depths at S1–S3 are 24.6 m, 35.7 m and 5.5 m, respectively. On 26 March, three hot wire thickness gauges were deployed in a triangular form at S2, for monitoring ice and snow thicknesses. Measurements lasted from 1 April to 20 December, at an interval of 1–3 days. On 27 March, a thermistor string, with specifications identical to the one at Lake Mochou, was deployed at S2 to measure the vertical temperature profile from ice cover to seawater. These measurements were taken from 1 April to 12 December, at an interval of 30 min.

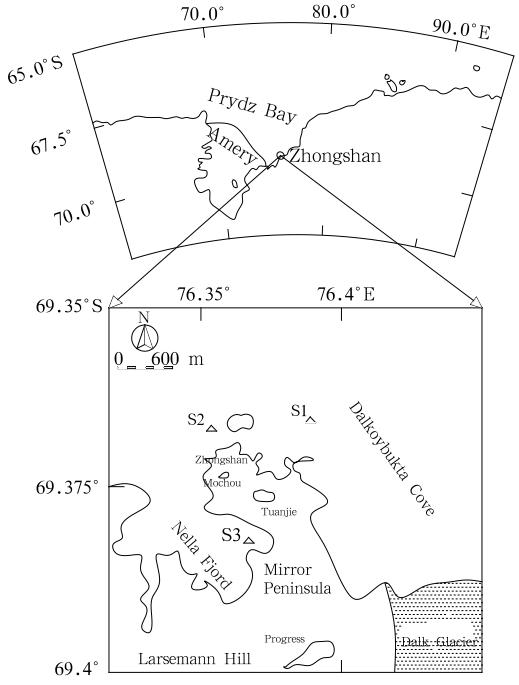

Figure 1 Locations of landfast ice and lake ice measurements around Zhongshan Station in 2006.

2 Results

2.1 Snow and ice thickness

Figure 2 shows time series of ice thickness at multiple sites and those of snow thickness over Lake Mochou and S2. Every snow depth peak in the time series may be associated with a snowfall event. During a snowfall event, wind speed was relatively weak, normally less than 4 $m \cdot s^{-1}$, although the speed would increase rapidly by the end of the snowfall event. Due to the snow blowing, snow depth at both Lake Mochou and S2 was very small throughout the experiment. Furthermore, lake ice surface was relatively slippery, resulting in a smaller snow depth at Mochou than that at S2.

Complete freeze up of Mochou, Tuanjie and Progress occurred on 27 February, 1 March and 24 February, respectively. The Freeze up date of lakes is related to local atmospheric forcing, heat storage in the lake during summer-fall, morphological properties of the lake and local topography[19]. The freeze up of the Lake Mochou occurred relatively early, which may be explained by its small size, and wind shields by hills and artificial structures around the lake. The freeze up of Lake Tuanjie occurred latest, because of its relatively large size and lack of the wind shields. The freeze up of the Lake Progress occurred earliest, which may be attributed to its location near the continental ice sheet. Ice growth rates at these lakes were very similar after the formation of a continuous ice sheet, until the end of July. Then the growth rate at Lake Mochou dramatically declined, producing the smallest ice thickness of all lakes. Annual maximal ice thickness appeared earliest at Lake Mochou, latest at Lake Progress. The smallest annual maximum ice thickness was at Lake Mochou. This might be attributed to the pump at the lake bottom, which may have produced a larger heat flux from the water to the ice bottom.

Continuous ice sheets occurred on 1 March, 5 March and 6 March at S1–S3, respectively. These dates were slightly later than those of the lakes, because of the lower freezing point of seawater. Nella Fjord is shallow and well sheltered from the ocean swell and prevailing winds. The S3 site froze 2–5 days earlier than other areas around Zhongshan Station (S1 and S2). Ice growth rates at S1–S3 were very similar after the continuous ice sheet formed, until the end of October. From then onward, the ice growth rate at S3 became smaller and ice thickness reached its annual maximum relatively earlier (30 October, 167 cm). This might be attributed to the shallow snow cover on the Larsemann Hills, where sand and small stones were swept onto the leeward side of the Mirror Peninsula, and deposited onto the ice surface of Nella Fjord. Surface deposits of sand and stones reduced albedo, promoting surface melt and ponding during late spring and summer. The ice growth rate at S1 and S2

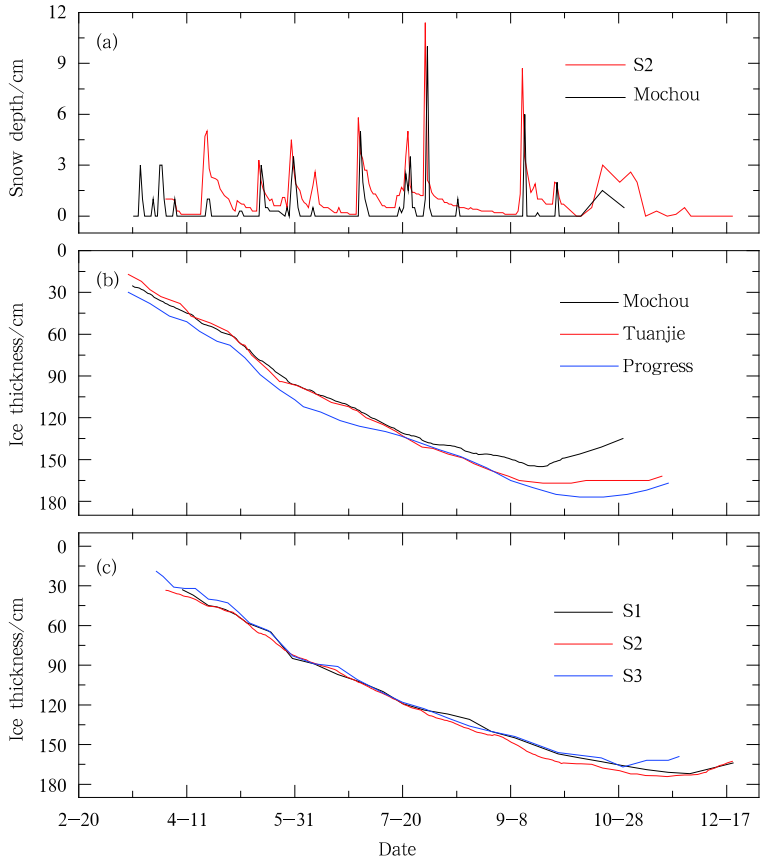

Figure 2 Variation in snow depth (a), lake-ice thickness (b), and landfast ice thickness (c) during 2006.

remained close during the entire experiment. Annual maximum ice thicknesses at both sites were reached by the end of November, with values of 172 cm and 174 cm, respectively. In other words, the landfast ice reached its annual maximum thickness about 1–2 months later than the lake ice around Zhongshan Station.

Figure 3 presents time series of ice growth rates at Lake Mochou and S2, along with their monthly average values. Generally speaking, the ice growth rates at Lake Mochou and S2 were similar throughout the entire experiment, and their correlation coefficient was 0.82 (P <0.01). Maximum ice growth rates at both sites occurred at the beginning of May, with values of 1.45 cm·d^{-1} and 1.35 cm·d^{-1}, respectively. From then onward, ice growth rates at both sites decreased with increasing ice thickness. From the end of July onward, the ice growth rate at Mochou decreased more rapidly than at S2, causing a greater deviation of rate between the sites. This resulted an earlier ice melting at Mochou. This could be related to a smaller extinction coefficient for lake ice[20−21], which would allow more solar radiation transferred through the lake ice cover after July, accelerating ice thaw.

2.2 Ice temperaturevertical profile and its response to surface ice temperature

Figure 4 shows the temporal evolution of internal ice temperature at Lake Mochou and S2. At both sites, the ice temperature in the top layer fluctuated greatly, in response to variations in surface air temperature. There was substantial attenuation and lag for the fluctuation at deeper layer, especially at S2. The temperature at ice bottom remained at the freezing point of local water at both sites. From mid September onward, ice temperature climbed as summer approached, which reduced the ice-temperature gradient at both sites. However, the increase in landfast ice temperature was greater than that of the lake ice. Interior melt of sea ice may result in desalination, which makes sea-ice melt to be different from that of lake ice. The desalination within sea ice may increase the ice melting point, elevating the ice temperature above the freezing point of local seawater.

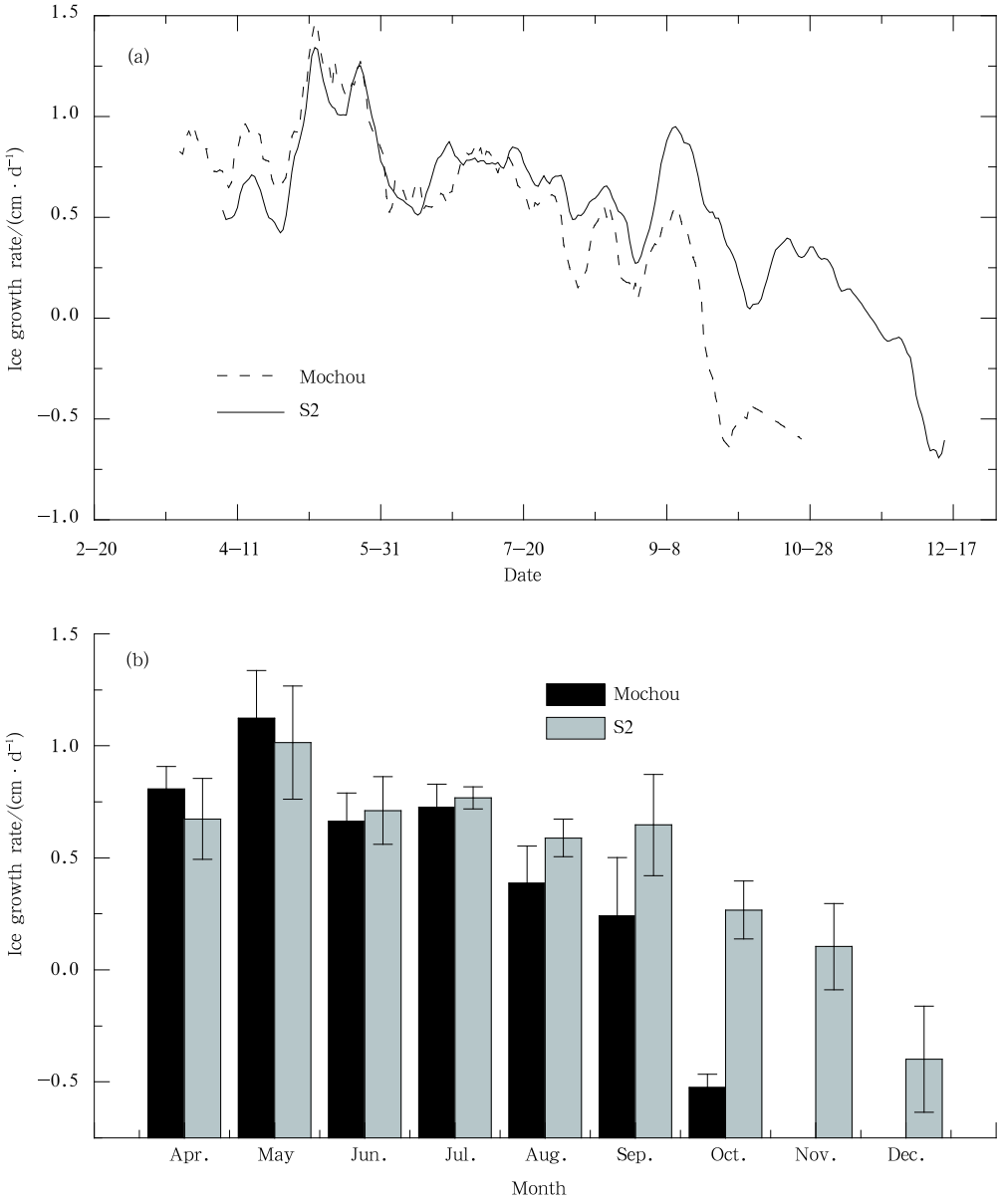

Figure 3 Growth rates of lake ice and landfast ice (a) and their monthly average values (b).

To quantify ice temperature variations at Lake Mochou and S2 in response to the daily changes in air temperature, we calculated the daily ice temperature changes at depths of –18 cm, –48 cm, –78 cm, –108 cm and –138 cm, for both Lake Mochou and S2. The 10-day mean calculated values are presented in Figure 5. Daily changes in ice temperatures decreased with increasing depth for both lake ice and landfast ice. At the same depth, however, the magnitudes of daily changes in lake ice temperatures were greater than those in landfast ice. This difference became more distinct with depth. The ratios between 10-day mean values of the daily variation of lake ice temperatures and those of landfast ice were 2.3, 2.8, 3.4, 5.0 and 8.8, for depths of –18 cm, –48 cm, –78 cm, –108 cm and –138 cm, respectively. The differences can be explained by the difference in composition between lake ice and sea ice. Sea ice is composed of pure ice crystals, brine, solid salt, air bubbles and other impurities. The outstanding difference between the compositions of lake fresh ice and sea ice is that there is no liquid or solid salt within the ice matrix. The phase fractions between liquid salt and solid salt within sea ice depend on in-situ ice temperatures. The changes in the phase fractions

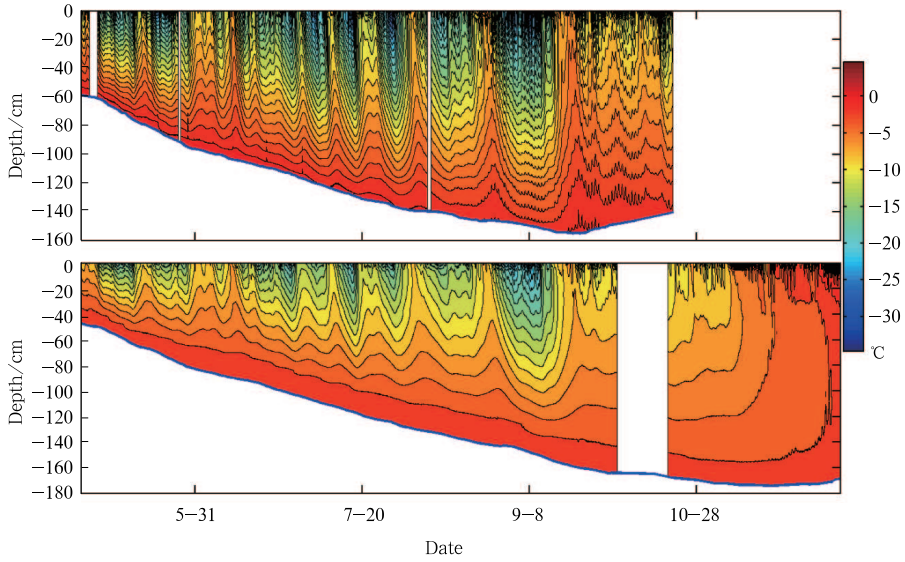

Figure 4 Evolution of internal temperature of lake ice at Lake Mochou (top), and of landfast ice at S2 (bottom); blue solid lines represent ice-water interfaces, and gaps represent intervals when no data were available.

may release or absorb some heat. Thus, daily changes in sea-ice temperatures were relatively weaker compared with those in lake ice, despite forcing by the same atmospheric conditions. Furthermore, the relatively heavy snow cover over S2 may have attenuated the daily changes in ice temperature there.

Figure 6 shows the vertical profiles of daily minimum and maximum ice temperature at Lake Mochou and S2, from 20 April through 20 September. The profiles again illustrated that lake ice temperature had larger daily variation than that of landfast ice. Because of a skeletal layer at the bottom of landfast ice, which was composed of a large fraction of brine[22], there was a 5–10 cm isothermal layer at the bottom of landfast ice. This layer did not appear in the lake ice.

We now quantify the temporal lag of ice temperature relative to those in surface air temperature. We calculated lag correlation coefficients between ice temperatures and surface air temperature, for two time windows: from 1 June to 15 July, the period during the polar night (period 1), and from 17 August to 30 September, the period after the polar night (period 2).

The calculations are shown in Figure 7. In period 1, the mean maximum lag correlation coefficient from the surface to a depth of –66 cm was 0.79±0.07 at Mochou, which was 1.3 times as that at S2, 0.60±0.13. The temporal lag according to the maximum lag correlation coefficient was 0.62±0.40 d at Mochou, which was 0.64 times that at S2, 0.98±0.71 d. This temporal lag at –66 cm depth was 1.2 d and 2.1 d for Mochou and S2, respectively. In period 2, the mean maximum lag correlation coefficient from the surface to a depth of –102 cm was 0.89±0.04 at Mochou, which was 1.2 times that at S2, 0.77±0.08. The temporal lag according to the maximum lag correlation coefficient was 1.20±0.80 d at Mochou, which was 0.49 times that at S2, 2.43±1.70 d. The temporal lags at –102 cm depth were 2.5 d and 5.4 d for Mochou and S2, respectively. The results from both periods indicate that the maximum lag correlation coefficients decreased linearly with depth (P <0.01), and the corresponding temporal lags increased linearly with depth (P <0.01) for both lake ice and landfast ice.

2.3 Conductive heat flux through the ice cover

Conductive heat flux through ice cover is the primary forcing for ice growth at the bottom. Vertical discontinuity of the conductive heat flux through ice cover is the crucial factor for interior ice melt. To quantify the vertical discontinuity of the conductive heat flux, we calculated the flux in the layers of –12 to –30 cm, –54 to –72 cm and –96 to –114 cm, for both Mochou and S2. The flux was calculated by

$$F_c = k_i \frac{\partial T_i}{\partial z_i} \quad (1)$$

where F_c is conductive heat flux, k_i is ice thermal

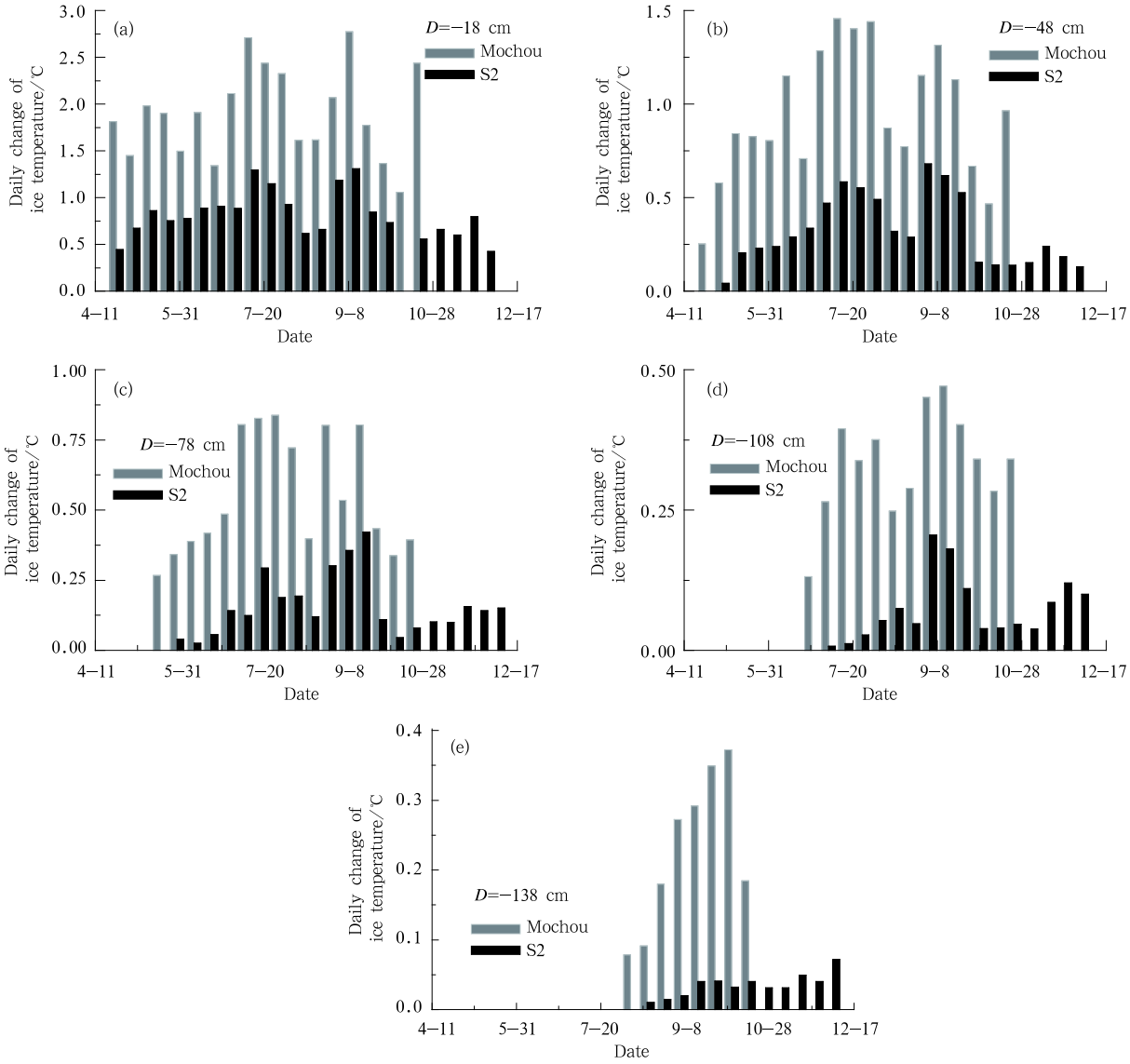

Figure 5 Daily variation of lake ice and landfast ice temperatures, at varying depths.

conductivity, which is a function of ice temperature and ice salinity[23−24], and $(\partial T_i/\partial z_i)$ is vertical ice temperature gradient. Figure 8 shows that the F_c through ice cover was primarily related to surface air temperature and ice thickness. Under the same surface air temperature, the F_c decreased with increasing ice thickness. There was a notable high-frequency oscillation in F_c through the top layer (–12 to –30 cm), especially for the sea ice at S2, similar to the time series of ice temperature. This high-frequency oscillation was compressed in the deeper layer. Under the same surface air temperature, the F_c through both the middle (–54 to –72 cm) and low (–96 to –114 cm) layers was smaller for sea ice than for lake ice. Also similar to the time series of ice temperature, there was a temporal lag between the low-frequency change of F_c at the middle/low layers and that at the top layer, especially for sea ice. The downward F_c (negative value) may occur at the top layer when the surface air temperature increases rapidly, which causes conductive heat to be concentrated in the subsurface layer of the ice column. Conductive heat flux slowed distinctly decrease when ice melt commenced, especially in the middle/low layer, because of the weak ice-temperature gradient. For the skeleton layer at the sea ice bottom, with substantial brine fraction and small ice-temperature gradient, the F_c at layers of –54 to –72 cm and –96 to –114 cm was small for sea ice, during which time the ice bottom immediately grew downward past the investigated layer.

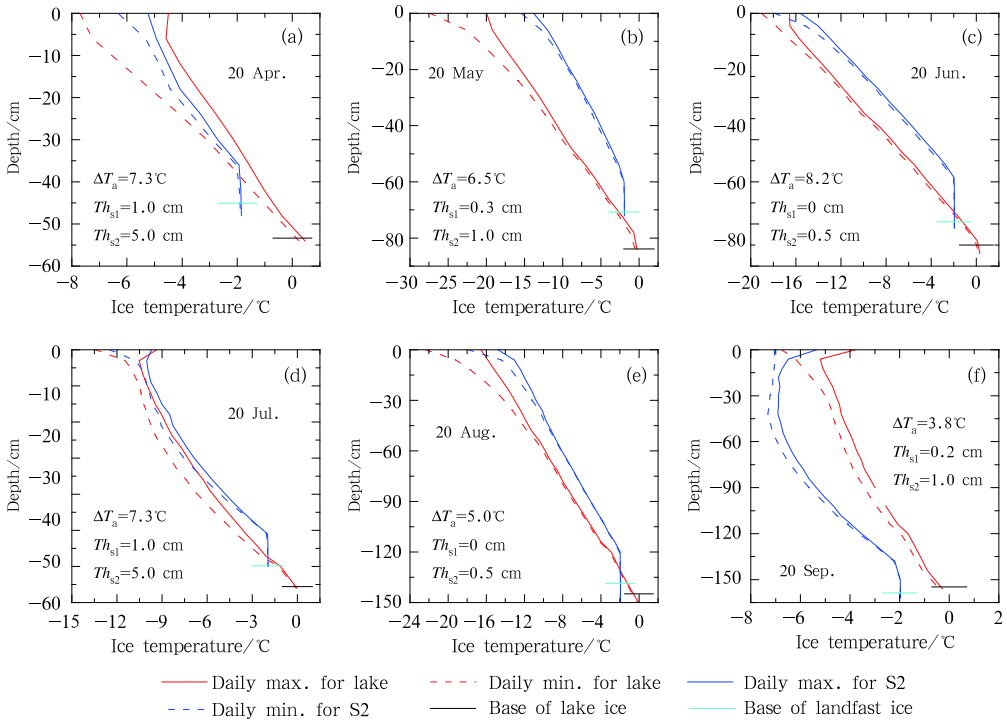

Figure 6 Vertical profiles of daily maximum and minimum temperatures of lake ice and sea ice; also shown are ΔT_a for daily variation of air temperature, and Th_{s1} and Th_{s2} for snow depths above lake ice and landfast ice.

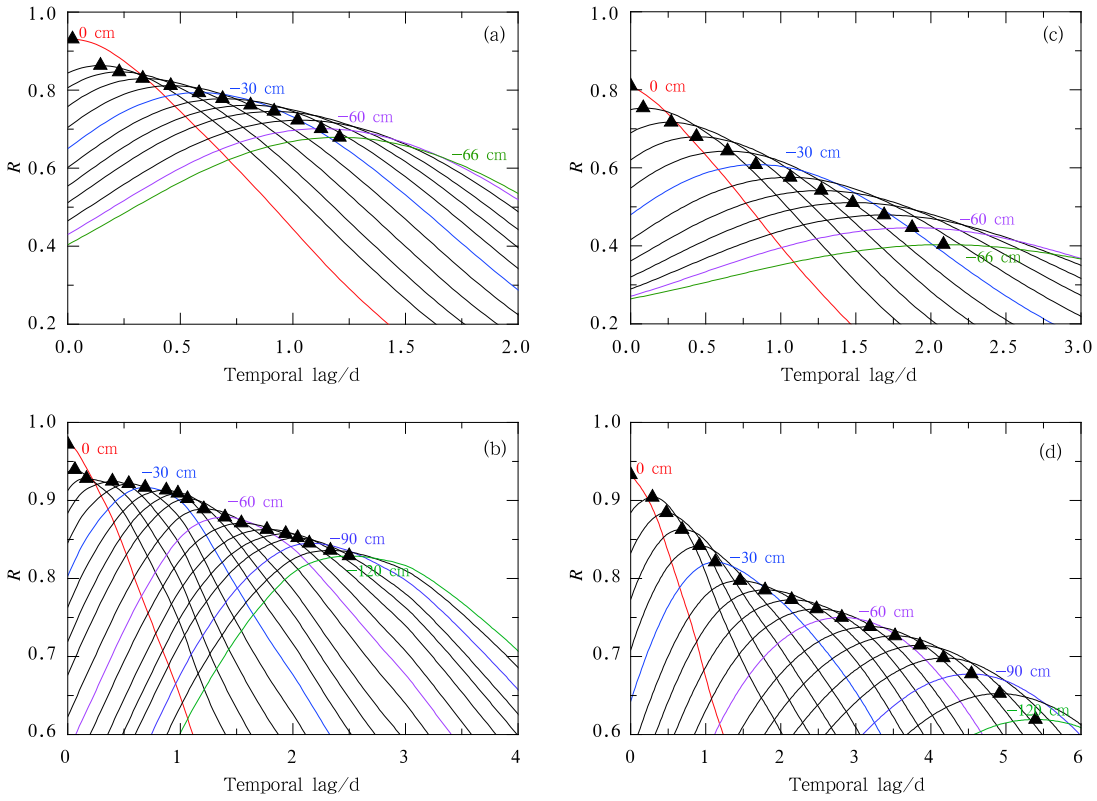

Figure 7 Lag correlation coefficients of ice temperatures at varying depths relative to air temperature: a and b for lake ice during periods 1 and 2, respectively, c and d for landfast ice during periods 1 and 2, respectively.

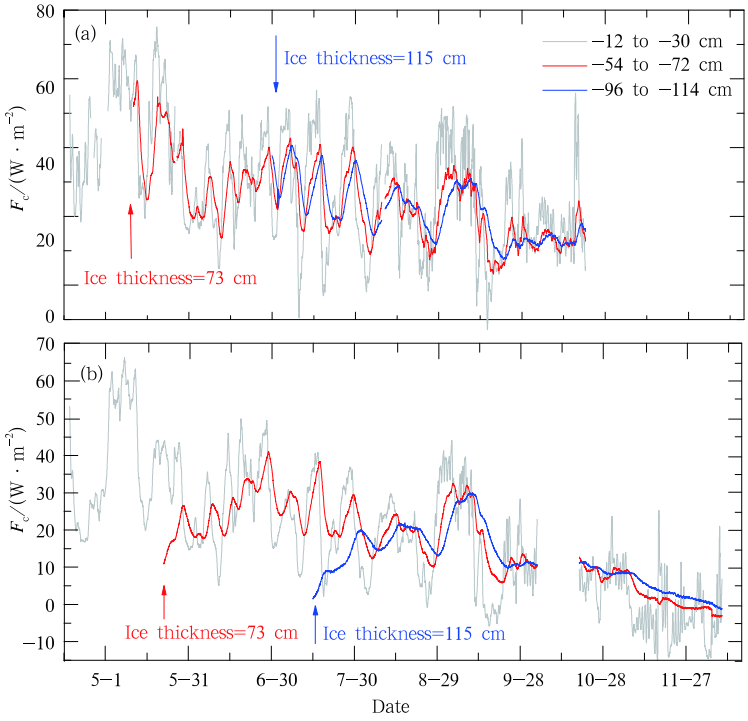

Figure 8 Variations in conductive heat flux at varying depths of lake ice (a) and landfast ice (b).

This reflects a sea-ice thermodynamic process that is different from lake ice.

3 Conclusions

A continuous ice sheet formed over the lakes and coastal regions around Zhongshan Station from later February to the beginning of March. The freeze date of the landfast ice was slightly later (about 0–6 d) than lake ice. The lake ice attained its annual maximum ice thickness from the end of September to the beginning of October, 1–2 months earlier than landfast ice. The annual maximum ice thickness was very similar for lake ice and landfast ice, ranging from 167 to 177 cm, except at Lake Mochou. The annual maximum ice thickness at Mochou was smallest, which might be attributable to the influence of a pump at the lake bottom.

Due to enwrapped brine and heavy snow over the surface, temporal variations in landfast ice temperature had a weaker response and a stronger temporal lag to temporal variations in surface air temperature, compared to lake ice. During the melt season, the sea ice temperature increased to warmer than the freezing point of local seawater, because of the interior desalination. This resulted in a weaker ice-temperature gradient and conductive heat flux than in lake ice.

Under the same atmospheric forcing, the lake/sea ice thermodynamic processes also may be influenced by the solar radiations absorbed by the ice column, and by the heat flux from the bottom water. Thus, optical and standard oceanographic measurements (e. g., turbulence measurements under the ice) still need to be made, in association with mass balance measurements for a thorough understanding of the thermodynamic processes of lake ice and landfast ice around Zhongshan Station.

Acknowledgments This work was supported by the National Basic Research Program of China(Grant no. 2010 CB950301), the China Postdoctoral Science Foundation (Grant no.20100470400), and the Shanghai Postdoctoral Sustentation Fund(Grant no. 11R21421800). We are grateful to Mr. Dong Li, Mr. Liu Xiufeng, Mr. Jin Wei, and Mr. Du Shuangzhi for their field support. We would like to acknowledge the meteorological station of Zhongshan for providing the atmospheric data.

References

1 Livingstone D M. Break-up dates of alpine lakes as proxy data for local and regional mean surface air temperatures. Climatic Change, 1997, 37: 407–439

2 Magnuson J J, Robertson D M, Benson B J, et al. Historical trends in lake and river ice cover in the Northern Hemisphere, Science. 2000, 289(5485): 1743–1746

3 Shirasawa K, Leppäranta M, Saloranta T, et al. The thickness of coastal fast ice in the Sea of Okhotsk.Cold Regions Science and Technology, 2005, 42(1): 25–40

4 Heil P. Atmospheric conditions and fast ice at Davis, East Antarctica: A case study. Journal Geophysical Research, 2006, 111, C05009, doi:10.1029/2005JC002904

5 Giles A B, Massom R A, Lytle V I. Fast-ice distribution in East Antarctica during 1997 and 1999 determined using RADARSAT data. Journal of Geophysical Research, 2008, 113, C02S14, doi:10. 1029/2007JC004139

6 Qin B, Huang Q. Evaluation of the climatic change impacts on the inland lake—a case study of LakeQinghai, China. Climatic Change, 1998, 39: 695–714

7 Leppäranta M, Reinart A, Erm A, et al. Investigation of ice and water properties and under-ice light fields in fresh and brackish water bodies. Nordic Hydrology, 2003, 34(3): 245–266

8 Mironov D, Terzhevik A, Kirillin G, et al. Radiatively driven convection in ice-covered lakes: Observations, scaling, and a mixed layer model. Journal of Geophysical Research, 2002, 107(C4), 3032, doi: 10.1029/2001JC000892

9 Livingstone D M. Lake oxygenation: application of a one-box model with ice cover. Internationale Revue der gesamten Hydrobiologie und Hydrographie, 1993, 78(4): 465–480

10 Gerten D, Adrian R. Climate-driven changes in spring plankton dynamics and the sensitivity of shallow polymictic lakes to the North Atlantic Oscillation. Limnology and Oceanography, 2000, 45(5): 1058–1066

11 Barica J, Mathias J A. Oxygen depletion and winterkill risk insmall prairie lakes under extended ice cover. Journal of the Fisheries Research Board of Canada, 1979, 36: 980–986

12 Li S K. Lakes of the Larsemann Hills, East Antarctica. Journal of Lake Sciences, 1995, 7(3): 193–202 (In Chinese)

13 Feng S Z, Xue Z, Chi W Q. Topographic features around Zhongshan Station, Southeast of Prydz Bay. Chinese Journal of Oceanology and Limnology, 2008, 26(4): 467–472, doi:10.1007/s00343-008-0467-8

14 Lei R B, Li Z J, Zhang Z H, et al. Summer fast ice evolution off Zhongshan Station, Antarctica. Chinese Journal of Polar Science, 2008, 19 (1): 54–62

15 Tang S L, Qin D H, Ren J W, et al. Structure, salinity and isotopic composition of multi-year landfast sea ice in Nella Fjord, Antarctica. Cold Regions Science and Technology, 2007, 49(2): 170–177

16 Lei R B, Li Z J, Cheng B, et al. Annual cycle of landfast sea ice in PrydzBay, east Antarctica. Journal of Geophysical Research, 2010, doi:10.1029/2008JC005223

17 Lei R B, Li Z J, Dou Y K, et al. Observations of the growth and decay processes of fast ice around Zhongshan Station in Antarctica. Advances in Water Science, 2010, 21(5): 708–712 (In Chinese)

18 Lei R B, Li Z J, Qin J M, et al. Investigation of new technologies for in-situ ice thickness observation. Advances in Water Science, 2009, 20(2): 287–292 (In Chinese)

19 Palecki M A, Barry R G. Freeze-up and break-up of lakes as an index of temperature changes during the transition seasons: A case study for Finland. Journal of Climate and Applied Meteorology, 1986, 25: 893–902

20 Arst H, Erm A, Leppäranta M, et al. Radiativecharacteristics of ice-covered fresh- and brackish-waterbodies. Proceedings of the Estonian Academy of Sciences-Geology, 2006, 55(1): 3–23

21 Lei R B, Leppäranta M, Erm A, et al. Field investigations of apparent optical properties of ice cover in Finnishand Estonian lakes in winter 2009. Estonian Journal of Earth Sciences, 2011, 60(1): 50–64

22 Eicken H. From the microscopic to the macroscopic to the regional scale: Growth, microstructure and properties of sea ice. In Thomas D, Dieckmann G S. Sea ice-an introduction to itsphysics, biology, chemistry and geology, Blackwell Science, London, 2003: 22–81

23 Untersteiner N. On the mass and heat budget of arctic sea ice. Meteorology and Atmospheric Physics, 1961, 12(2): 150–182

24 Yen Y C. Review of thermal properties of snow, ice and seaice.Cold Regions Research and Engineering Laboratory Report 81–10, Hanover, New Hampshire, 1981: 1–27